Subwavelength slow-light waveguides based on a plasmonic analogue of electromagnetically induced transparency

Yin Huang,[1] Changjun Min,[2] and Georgios Veronis[1,2,a)]
[1]*Department of Electrical and Computer Engineering, Louisiana State University, Baton Rouge, Louisiana 70803, USA*
[2]*Center for Computation and Technology, Louisiana State University, Baton Rouge, Louisiana 70803, USA*

(Received 6 May 2011; accepted 20 September 2011; published online 7 October 2011)

We introduce a plasmonic waveguide system, based on a plasmonic analogue of electromagnetically induced transparency, which supports a subwavelength slow-light mode, and exhibits a small group velocity dispersion. The system consists of a periodic array of two metal-dielectric-metal (MDM) stub resonators side-coupled to a MDM waveguide. Decreasing the frequency spacing between the two resonances increases the slowdown factor and decreases the bandwidth of the slow-light band. We also show that there is a trade-off between the slowdown factor and the propagation length of the slow-light mode. © *2011 American Institute of Physics*. [doi:10.1063/1.3647951]

Plasmonic waveguides have shown the potential to guide and manipulate light at deep subwavelength scales.[1] Slowing down light in plasmonic waveguides leads to enhanced light-matter interaction and could therefore enhance the performance of nanoscale plasmonic devices such as switches and sensors.[2–8] Among the different plasmonic waveguiding structures, metal-dielectric-metal (MDM) plasmonic waveguides are of particular interest because they support modes with deep subwavelength scale over a very wide range of frequencies extending from DC to visible.[9] We recently introduced a MDM plasmonic waveguide system, based on a plasmonic analogue of periodically loaded transmission lines, which supports a guided subwavelength slow-light mode.[8]

In this letter, we introduce an alternative MDM plasmonic waveguide system, based on a plasmonic analogue of electromagnetically induced transparency (EIT), which also supports a guided subwavelength slow-light mode. EIT is a coherent process observed in three-level atomic media, which allows a narrow transparency window in the spectrum of an otherwise opaque medium and can slow down light pulses by several orders of magnitude.[10] Since the EIT spectrum results from the interference of resonant pathways,[10,11] it has been recognized that similar interference effects can also occur in classical systems, such as optical waveguides coupled to resonators and metamaterials.[10,12–14] In addition, it has been demonstrated that periodic optical waveguides, resulting from cascading structures with EIT-like response, can slow down and even stop light.[11,15,16]

Our proposed structure consists of a periodic array of two MDM stub resonators side-coupled to a MDM waveguide. Side-coupled-cavity structures have been previously proposed as compact filters, reflectors, switches, and impedance matching elements for plasmonic waveguides.[17–20] Here, we show that the proposed structure supports a band diagram similar to that of EIT systems, with three photonic bands in the vicinity of the two stub resonances. The middle band corresponds to a mode with slow group velocity and zero group velocity dispersion near the middle of this band. We find that decreasing the frequency spacing between the resonances increases the slowdown factor and decreases the bandwidth of the middle band. We also show that there is a trade-off between the slowdown factor and the propagation length of the supported optical mode in such slow-light plasmonic waveguide systems.

We use a finite-difference frequency-domain (FDFD) method to investigate the properties of the structure.[8] This method allows us to directly use experimental data for the frequency-dependent dielectric constant of metals such as silver,[21] including both the real and imaginary parts, with no approximation. Perfectly matched layer (PML) absorbing boundary conditions are used at all boundaries of the simulation domain. When simulating the periodic waveguiding structure, we place several periods of the structure within the PML layer to drastically reduce spurious reflections at PML interfaces.[8]

We first consider a plasmonic MDM waveguide side-coupled to two MDM stub resonators (Fig. 1(a)). The resonant frequencies of the cavities can be tuned by adjusting the cavity lengths L_1 and L_2. This system is a plasmonic analogue of EIT.[22,23] The MDM waveguide and MDM stub resonators have deep subwavelength widths ($w \ll \lambda$), so that only the fundamental TM mode is propagating. Thus, we can use single-mode scattering matrix theory to account for the behavior of the system.[24] The complex magnetic field reflection coefficient r_1 and transmission coefficients t_1, $t_2 = t_3$ for the fundamental propagating TM mode at a MDM waveguide crossing (Fig. 1(b)) as well as the reflection coefficient r_2 at the boundary of a short-circuited MDM waveguide (Fig. 1(c)) are numerically extracted using FDFD.[24] The power transmission spectra $T(\omega)$ of the two-cavity system (Fig. 1(a)) can then be calculated using scattering matrix theory as

$$T = |t_1 - C|^2, \tag{1}$$

a)Electronic mail: gveronis@lsu.edu.

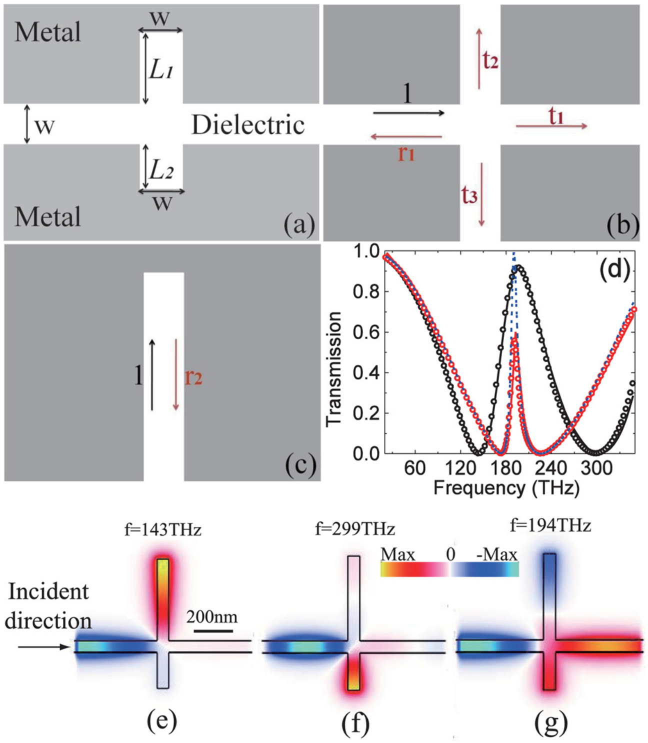

FIG. 1. (Color online) (a) Schematic of a MDM plasmonic waveguide side-coupled to two MDM stub resonators. (b) Schematic defining the reflection coefficient r_1, and transmission coefficients t_1, t_2, t_3 when the fundamental TM mode of the MDM waveguide is incident at a waveguide crossing. Note that $t_2 = t_3$ due to symmetry. (c) Schematic defining the reflection coefficient r_2 of the fundamental TM mode of the MDM waveguide at the boundary of a short-circuited MDM waveguide. (d) Transmission spectra for the structure of (a) calculated using FDFD (circles) and scattering matrix theory (solid line) for a silver-air structure with $w = 50$ nm. Results are shown for $L_1 = 360$ nm, $L_2 = 160$ nm (black line and circles) and $L_1 = 295$ nm, $L_2 = 220$ nm (red line and circles). Also shown are the transmission spectra calculated using FDFD for $L_1 = 295$ nm, $L_2 = 220$ nm, and lossless metal (blue dashed line). (e)-(g) Magnetic field profiles for the structure of (a) for $L_1 = 360$ nm, $L_2 = 160$ nm, $w = 50$ nm at $f = 143$, 299, 194 THz, when the fundamental TM mode of the MDM waveguide is incident from the left.

which is in excellent agreement with the exact results obtained using FDFD (Fig. 1(d)). Here, $C = \frac{t_2^2(2t_1 - 2r_1 + s_1 + s_2)}{t_1^2 - (r_1 - s_1)(r_1 - s_2)}$, $s_i = r_2^{-1}\exp(2\gamma_{\mathrm{MDM}} L_i)$, $i = 1$, 2, and $\gamma_{\mathrm{MDM}} = \alpha_{\mathrm{MDM}} + i\beta_{\mathrm{MDM}}$ is the complex wave vector of the fundamental propagating TM mode in a MDM waveguide of width w.

The transmission spectra $T(\omega)$ feature two dips (Fig. 1(d)). We found that the frequencies ω_1, ω_2 where these dips occur are approximately equal to the first resonant frequencies of the two cavities, i.e., $\phi_{r_1}(\omega_i) + \phi_{r_2}(\omega_i) - 2\beta_{\mathrm{MDM}}(\omega_i)L_i \approx -2\pi$, $i = 1, 2$, where $\phi_{r_i} = \arg(r_i)$, $i = 1, 2$. When either one of the cavities is resonant, the field intensity in that cavity is high, while the field intensity in the other cavity is almost zero, since it is far from resonance (Figs. 1(e) and 1(f)). In addition, the transmission is almost zero, since the incoming wave interferes destructively with the decaying amplitude into the forward direction of the resonant cavity field. The transmission spectra $T(\omega)$ also feature a transparency peak centered at frequency ω_0. We found that ω_0 is approximately equal to the first resonant frequency of the composite cavity of length $L_1 + L_2 + w$ formed by the two cavities, i.e., $2\phi_{r_2}(\omega_0) - 2\beta_{\mathrm{MDM}}(\omega_0)(L_1 + L_2 + w) \approx -2\pi$.

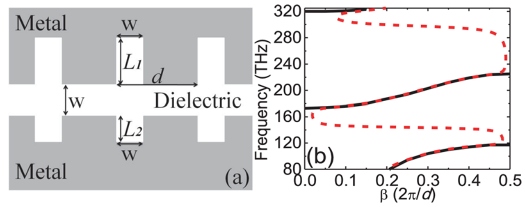

FIG. 2. (Color online) (a) Schematic of a plasmonic waveguide system consisting of a periodic array of two MDM stub resonators side-coupled to a MDM waveguide. (b) Dispersion relation of the plasmonic waveguide system of (a) calculated using FDFD (red dashed line). Results are shown for a silver-air structure with $d = 300$ nm, $L_1 = 360$ nm, $L_2 = 160$ nm, and $w = 50$ nm. Also shown is the dispersion relation for lossless metal (black solid line).

Thus, the transmission peak frequency ω_0 is tunable through the cavity lengths L_1, L_2. When $\omega = \omega_0$, the field intensity is high in the entire composite cavity (Fig. 1(g)), and the transmission spectra exhibit a peak due to resonant tunneling of the incoming wave through the composite cavity. The width of the peak is highly sensitive to the frequency spacing between the resonances $\delta\omega = \omega_2 - \omega_1$, which can be tuned by adjusting the stub lengths difference $\delta L = L_1 - L_2$. As $\delta\omega$ decreases, the width of the peak decreases (Fig. 1(d)). In the lossless metal case, the center peak can be tuned to be arbitrarily narrow with unity peak transmission (Fig. 1(d)). In the presence of loss, the peak transmission decreases, as the frequency spacing $\delta\omega$ decreases (Fig. 1(d)).

We next consider the plasmonic waveguide system (Fig. 2(a)) obtained by periodically cascading the side-coupled-cavity structure of Fig. 1(a). The periodicity d is subwavelength ($d \ll \lambda$), so that the operating wavelength is far from the Bragg wavelength of the waveguide[8] ($\lambda \gg \lambda_{\mathrm{Bragg}}$). In addition, the distance between adjacent side-coupled cavities $d - w$ is chosen large enough so that direct coupling between the cavities has a negligible effect on the dispersion relation of the system.[8] Using single-mode scattering matrix theory,[24] the dispersion relation between the frequency ω and the Bloch wave vector $\gamma = \alpha + i\beta$ of the entire system is found to be

$$\cosh(\gamma d) = \frac{A}{2}\exp[-\gamma_{\mathrm{MDM}}(d - w)] + \frac{B}{2}\exp[\gamma_{\mathrm{MDM}}(d - w)], \tag{2}$$

which is in excellent agreement with the exact results obtained using FDFD (Fig. 3(a)). Here, $A = (t_1 - r_1)\frac{t_1 + r_1 - 2C}{t_1 - C}$ and $B = (t_1 - C)^{-1}$. In Fig. 2(b), we show the dispersion relation for the plasmonic waveguiding structure of Fig. 2(a). In the lossless metal case, the system supports three photonic bands in the vicinity of the cavity resonances. The middle band corresponds to a mode with slow group velocity $v_g \equiv \frac{\partial\omega}{\partial\beta}$ and zero group velocity dispersion $\beta_2 \equiv \frac{\partial^2\beta}{\partial\omega^2}$ near the middle of this band (Fig. 2(b)). In the two band gaps between the three bands the system supports non-propagating modes with $\beta = 0$. Such a band diagram is similar to that of EIT systems.[15] When losses in the metal are included, the band structure is unaffected in the frequency range of the three bands except at the band edges (Fig. 2(b)). In addition, in the frequency range of the two band gaps, the Bloch wave vector γ has an imaginary component ($\beta \neq 0$), and the dispersion

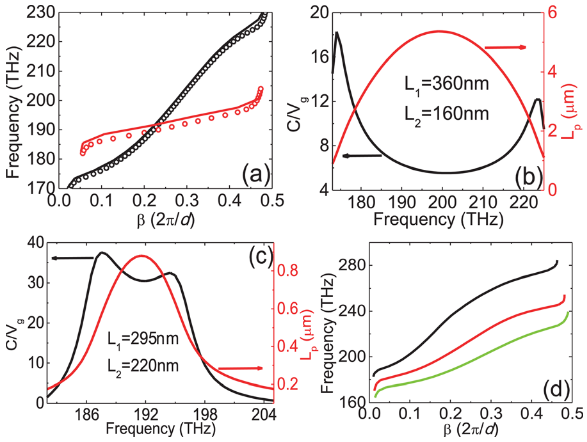

FIG. 3. (Color online) (a) Dispersion relation of the plasmonic waveguide system of Fig. 2(a) calculated using FDFD (circles) and scattering matrix theory (solid line). Results are shown for $L_1 = 360$ nm, $L_2 = 160$ nm (black line and circles), and $L_1 = 295$ nm, $L_2 = 220$ nm (red line and circles). All other parameters are as in Fig. 2(b). In both cases, only a portion of the band structure is shown, corresponding to the frequency range of the middle band. (b)-(c) Reciprocal of the group velocity v_g and propagation length L_p for the plasmonic waveguide system of Fig. 2(a) as a function of frequency calculated using FDFD. Results are shown for $L_1 = 360$ nm, $L_2 = 160$ nm, and $L_1 = 295$ nm, $L_2 = 220$ nm. All other parameters are as in Fig. 2(b). (d) Dispersion relation of the plasmonic waveguide system of Fig. 2(a) calculated using FDFD. Results are shown for $d = 100$ nm (black line), $d = 200$ nm (red line), and $d = 300$ nm (green line). All other parameters are as in Fig. 2(b). In all cases, only a portion of the band structure is shown, corresponding to the frequency range of the middle band.

relation experiences back-bending[8] with negative group velocity.

In addition, the width of the middle band and the slowdown factor c/v_g strongly depend on the frequency spacing between the resonances $\delta\omega = \omega_2 - \omega_1$. By decreasing the stub lengths difference δL, $\delta\omega$ decreases, and this leads to decreased bandwidth of the middle band (Fig. 3(a)). In Figs. 3(b) and 3(c), we show the slowdown factor c/v_g, and propagation length L_p for the plasmonic waveguide system of Fig. 2(a) as a function of frequency for two different values of δL. In both cases, we show the frequency range corresponding to the middle band of the system. For a given δL, the propagation length L_p of the supported optical mode is maximized at a frequency very close to the frequency where the group velocity dispersion is zero. As δL and therefore $\delta\omega$ decrease, the slowdown factor c/v_g increases, while the propagation length L_p decreases at the frequency of zero group velocity dispersion. Thus, there is a trade-off between the slowdown factor c/v_g and the propagation length L_p of the supported optical mode in such slow-light plasmonic waveguide systems.[8] For $\delta L = 200$ nm ($\delta L = 75$ nm), we have $c/v_g \simeq 6$ ($c/v_g \simeq 30$) at the frequency where the group velocity dispersion is zero (Figs. 3(b) and 3(c)). We found that even larger slowdown factors can be obtained by further decreasing δL at the cost of reduced propagation length. We also note that the propagation length of the system for a given slowdown factor can be increased by incorporating gain media in the structure.[25]

We also consider the effect of the periodicity d (Fig. 2(a)) on the dispersion relation of the system (Fig. 3(d)). For large d, the distance $d - w$ between adjacent two-cavity structures in the periodic waveguide is large, so that their coupling through the MDM waveguide is weak. In this regime, the frequency range of the middle band of the periodic waveguide system of Fig. 2(a) approximately corresponds to the frequency range of the transparency peak of the two-cavity structure of Fig. 1(a). As d decreases, the coupling between adjacent two-cavity structures increases. As a result, the slow-light middle band shifts to higher frequencies, while its width slightly broadens (Fig. 3(d)). Thus, the periodicity provides us an additional degree of freedom to tune the dispersion relation of the periodic waveguide system.

In conclusion, we introduced subwavelength slow-light waveguides for enhanced light-matter interaction, based on a plasmonic analogue of EIT. Unlike previously proposed structures,[8] such waveguides exhibit a small group velocity dispersion and a large slowdown factor over a broad wavelength range, features which are highly desirable for practical applications of slow-light devices.[26] In addition, if these waveguides are combined with gain and tunable refractive index materials, they could enable stopping and storing light in a subwavelength volume.[11]

This research was supported by the Louisiana Board of Regents (contracts LEQSF(2009-12)-RD-A-08 and NSF(2010)-PFUND-187).

[1] W. L. Barnes, A. Dereux, and T. W. Ebbesen, Nature **424**, 824 (2003).
[2] A. Karalis, E. Lidorikis, M. Ibanescu, J. Joannopoulos, and M. Soljacic, Phys. Rev. Lett. **95**, 063901 (2005).
[3] M. Sandtke and L. Kuipers, Nature Photon. **1**, 573 (2007).
[4] Z. Kang, W. Lin, and G. P. Wang, J. Opt. Soc. Am. B **26**, 1944 (2009).
[5] Q. Gan, Y. J. Ding, and F. J. Bartoli, Phys. Rev. Lett. **102**, 056801 (2009).
[6] A. Kocabas, S. S. Senlik, and A. Aydinli, Phys. Rev. Lett. **102**, 063901 (2009).
[7] E. Feigenbaum and M. Orenstein, Opt. Express **17**, 2465 (2009).
[8] L. Yang, C. Min, and G. Veronis, Opt. Lett. **35**, 4184 (2010).
[9] E. N. Economou, Phys. Rev. **182**, 539 (1969).
[10] P. Tassin, L. Zhang, T. Koschny, E. N. Economou, and C. M. Soukoulis, Phys. Rev. Lett. **102**, 053901 (2009).
[11] S. Fan, M. F. Yanik, Z. Wang, S. Sandhu, and M. L. Povinelli, J. Lightwave Technol. **24**, 2293 (2006).
[12] S. Zhang, D. A. Genov, Y. Wang, M. Liu, and X. Zhang, Phys. Rev. Lett. **101**, 047401 (2008).
[13] N. Papasimakis, V. A. Fedotov, and N. I. Zheludev, Phys. Rev. Lett. **101**, 253903 (2008).
[14] N. Liu, L. Langguth, T. Weiss, J. Kstel, M. Fleischhauer, T. Pfau, and H. Giessen, Nature Mater. **8**, 758 (2009).
[15] M. F. Yanik, W. J. Suh, Z. Wang, and S. Fan, Phys. Rev. Lett. **93**, 233903 (2004).
[16] Q. Xu, S. Sandhu, M. Povinelli, J. Shakya, S. Fan, and M. Lipson, Phys. Rev. Lett. **96**, 123901 (2006).
[17] Y. Matsuzaki, T. Okamoto, M. Haraguchi, M. Fukui, and M. Nakagaki, Opt. Express **16**, 16314 (2008).
[18] X. S. Lin and X. G. Huang, Opt. Lett. **33**, 2874 (2008).
[19] J. Liu, G. Fang, H. Zhao, Y. Zhang, and S. Liu, Opt. Express **17**, 20134 (2009).
[20] C. Min and G. Veronis, Opt. Express **17**, 10757 (2009).
[21] E. D. Palik, *Handbook of Optical Constants of Solids* (Academic, New York, 1985).
[22] R. D. Kekatpure, E. S. Barnard, W. Cai, and M. L. Brongersma, Phys. Rev. Lett. **104**, 243902 (2010).
[23] Z. Han and S. I. Bozhevolnyi, Opt. Express **19**, 3251 (2011).
[24] S. E. Kocabas, G. Veronis, D. A. B. Miller, and S. Fan, IEEE J. Sel. Top. Quantum Electron. **14**, 1462 (2008).
[25] S. A. Maier, *Plasmonics: Fundamentals and Applications* (Springer, New York, 2007).
[26] J. B. Khurgin, Adv. Opt. Photon. **2**, 287 (2010).